White Rose Research Online

eprints@whiterose.ac.uk
https://eprints.whiterose.ac.uk
Universities of Leeds, Sheffield and York

Deposited via The University of Sheffield.

White Rose Research Online URL for this paper:
https://eprints.whiterose.ac.uk/id/eprint/247257/

Version: Accepted Version

Article:
He, Z., Cai, C. and Rui, J. (2026) Perceived safety and crime risk across day and night contexts in Shanghai. Journal of Geovisualization and Spatial Analysis, 10 (2). 48. ISSN: 2509-8810

https://doi.org/10.1007/s41651-026-00291-2

© 2026 The Authors. Except as otherwise noted, this author-accepted version of a journal article published in Journal of Geovisualization and Spatial Analysis is made available via the University of Sheffield Research Publications and Copyright Policy under the terms of the Creative Commons Attribution 4.0 International License (CC-BY 4.0), which permits unrestricted use, distribution and reproduction in any medium, provided the original work is properly cited. To view a copy of this licence, visit http://creativecommons.org/licenses/by/4.0/

Reuse
This article is distributed under the terms of the Creative Commons Attribution (CC BY) licence. This licence allows you to distribute, remix, tweak, and build upon the work, even commercially, as long as you credit the authors for the original work. More information and the full terms of the licence here: https://creativecommons.org/licenses/

Takedown
If you consider content in White Rose Research Online to be in breach of UK law, please notify us by emailing eprints@whiterose.ac.uk including the URL of the record and the reason for the withdrawal request.

UNIVERSITY OF LEEDS
University of Sheffield
UNIVERSITY of York

Perceived Safety and Crime Risk Across Day and Night Contexts in Shanghai

Abstract

Safety perception plays a crucial role in promoting sustainable urban development, as it influences residents' spatial use behaviors, social interaction patterns, and neighborhood cohesion. However, existing studies have largely focused on single temporal contexts or relied on perception data derived from Western urban environments, leaving day–night differences in the relationship between safety perception and crime risk insufficiently understood. This study integrates generative artificial intelligence with questionnaire-based perception ratings to examine differences in safety perception between daytime and nighttime and their associations with crime risk. Focusing on central Shanghai, we analyzed adjudicated and publicly disclosed criminal cases from 2017 to 2019, generated corresponding nighttime street-view images (SVI) using a CycleGAN-based Day-to-Night (D2N) model, and obtained safety perception ratings for 1,751 valid SVI samples through a survey of 65 Shanghai residents. We then employed graph convolutional neural network weighted regression (GCNNWR) and bootstrap-based mediation analysis to examine the relationships between daytime and nighttime crime rates and related factors. The results show that the mean safety perception score decreased from 6.29 during daytime to 6.02 at nighttime, with low nighttime safety perception exhibiting more pronounced spatial clustering. Activity density was positively associated with crime rates, whereas the negative association between police facilities and crime rates weakened at night. In addition, TCI and LSU exhibited indirect pathways associated with nighttime crime rates through safety perception. These findings provide empirical support for incorporating nighttime safety experiences into urban safety governance and for implementing more temporally and spatially targeted governance strategies.

Keywords: Perceived safety; Crime risk; Day-night contexts; Crime prevention

1. Introduction

1.1 From crime control to perceived safety

The United Nations' Sustainable Development Goal 16 (SDG 16) explicitly calls for reducing violence and crime in order to promote safe and peaceful societies (Nations, 2025). Public safety is not only a prerequisite for sustainable urban development but also a fundamental condition for maintaining residents' well-being and social cohesion (Roy & Chowdhury, 2025). With accelerating urbanization and increasing social differentiation, urban safety has gradually extended beyond the traditional domain of law enforcement and crime control, evolving into a complex social condition jointly shaped by spatial environments, social structures, and individual perceptions

(McClanahan et al., 2024).

The impacts of crime extend far beyond direct victimization. Previous studies showed that fear of crime and feelings of uncertainty significantly influenced residents' everyday spatial behavior by discouraging the use of public spaces, encouraging avoidance of certain areas, and weakening community interactions. Over time, these processes accumulated and generated new forms of social inequality in daily life (Kounadi et al., 2025; Mandalapu et al., 2023; Navarrete-Hernandez et al., 2023). Therefore, relying solely on objective crime statistics is insufficient to fully understand urban safety. A critical challenge is to examine the relationship between subjective perceptions of safety and crime risks across day-night contexts, as well as their spatial variations.

1.2 Urban spatial environments, visual environments, and crime risk

The relationship between urban environments and crime has long attracted scholarly attention. Early research demonstrated that crime is spatially concentrated rather than randomly distributed across cities (Shaw & Moore, 1931). Crime Prevention Through Environmental Design (CPTED) subsequently emphasized that spatial configuration and environmental design can influence opportunities for crime by shaping visibility, access control, territoriality, and surveillance (Jeffery, 1971). Routine activity theory provides a complementary explanation by proposing that crime depends on the spatiotemporal convergence of suitable targets, motivated offenders, and the absence of capable guardians (Cohen & Felson, 1979). Together, these perspectives suggest that urban environments can influence crime by modifying opportunity structures, patterns of activity, and the conditions under which guardianship operates.

Empirical research found that areas with high pedestrian flows, such as commercial centers and transportation hubs, often exhibited more complex opportunity structures for crime (Anderson, 2007; Mao et al., 2021). Socioeconomic conditions also played an important role. For example, neighborhood poverty, social isolation, and demographic disparities were consistently associated with higher crime rate (Pantazis & Gordon, 2018; Stabile, 2023).

As research progressed, increasing attention shifted from objective crime incidents to residents' subjective perceptions of safety. Environmental conditions such as inadequate lighting, spatial enclosure, limited visibility, and poor maintenance have been associated with greater fear and lower safety perception (Rader et al., 2007; You et al., 2026). Safety perception is not merely a passive response to environmental conditions but may also influence spatial behavior. Fear of crime can lead individuals to restrict activities, avoid unsafe places, and adopt precautionary behaviors (Jackson & Gray, 2010; Liska et al., 1987), while longitudinal evidence suggests that heightened fear is associated with reduced neighborhood walking (Foster et al., 2014). These

behavioral adjustments may alter routine activities, target exposure, and informal guardianship, thereby affecting crime opportunities. Accordingly, safety perception can be conceptualized as a potential mediator linking visible environmental characteristics with crime risk.

More recently, advances in computer vision and big data enabled researchers to use Street View Images (SVI) to quantify urban visual characteristics and predict perceptual evaluations using machine learning (Li et al., 2015). The MIT Place Pulse dataset further supported this research by providing large-scale online ratings across perceptual dimensions such as safety, liveliness, beauty, and wealth, which were widely used to train deep learning models for streetscape perception (Lou et al., 2024). Building on these methods, studies increasingly examined relationships between visual environments and crime. For example, Zhang et al. (2021) and Gu et al. (2026) identified substantial mismatches between perceived safety and crime distributions in Houston and Beijing. Related studies in Sweden (Abraham et al., 2025), Ohio (Zhou et al., 2024), New York (He et al., 2025) and London (Liu et al., 2023) further demonstrated the applicability of these approaches across diverse urban contexts.

Although these studies provided valuable insights into urban visual environments and perceived safety, they relied predominantly on daytime SVI. This strong daytime bias limits the generalizability of existing findings, particularly in high-density urban environments.

1.3 Nighttime environments, visual data, and research challenges

The transition from day to night can substantially reshape urban visibility and patterns of human activity, thereby influencing both crime risk and perceived safety (Son et al., 2023; Ye et al., 2025). Routine activities theory and the guardianship hypothesis suggest that increases in crime occur when the dynamic balance between “suitable targets” and “capable guardians” is disrupted (Cohen & Felson, 1979; Hollis-Peel et al., 2011). After nightfall, reduced illumination and declining pedestrian flows weaken both visibility and natural surveillance, creating conditions that facilitate criminal activities. As a result, urban spaces such as transportation hubs (Ceccato et al., 2022), abandoned buildings (Haleem et al., 2021), and poorly lit streets (Block, 2024; Roy & Chowdhury, 2025) are more likely to become potential crime hotspots, increasing the overall probability of crime occurrence (Domínguez & Asahi, 2023).

Although SVI has been widely used to quantify urban visual environments and assess spatial perceptions, research in nighttime contexts remains limited. One major reason is the scarcity of nighttime SVI data at the city scale. For example, nighttime images account for only about 3% of all records in the Mapillary database (Y. Wang et al., 2026). This data limitation has significantly constrained systematic investigations of nighttime visual environments and their relationship with perceived safety (Fan &

Biljecki, 2024).

To address this limitation, recent advances in generative artificial intelligence have provided new opportunities for constructing nighttime streetscapes. Models such as CycleGAN can achieve high-accuracy transformations between daytime and nighttime images (Dou, 2025). Building on this capability, Z. Liu et al. (2024) trained a day-to-night (D2N) model to convert daytime SVI from multiple cities into nighttime imagery. Ye et al. (2025) further collected approximately 1,000 paired daytime and nighttime SVI from Hong Kong and Shanghai, combined generative transformation with perception surveys from 46 participants, and found that nighttime conditions generally reduced perceived safety. Similarly, Y. Wang et al. (2026) used approximately 2,000 paired day-night SVI samples from Boston to generate nighttime scenes and examine streetscape effects, showing that greenery improved perceived safety during the daytime but could reduce it at night, while lighting intensity produced heterogeneous effects.

Despite these advances, existing studies have primarily focused on methodological feasibility and preliminary differences in safety perception. The systematic integration of spatiotemporal crime patterns, streetscape environmental characteristics, and residents' subjective safety perceptions remains limited. This gap constrains our understanding of the mechanisms shaping nighttime urban safety and limits the development of a more comprehensive framework linking environmental design, crime risk, and urban governance.

1.4 Research gaps and our aim

Recent studies reveal four major gaps in the existing literature. First, differences in perceived safety between daytime and nighttime environments remain underexplored, with limited empirical examination based on residents' subjective perceptions and rating data. Second, prior research has not adequately identified the spatial correspondence between perceived safety and crime patterns across different times of day, nor has it systematically examined their potential misalignment. Third, existing analytical frameworks rarely integrate daytime and nighttime crime rate with subjective safety perceptions, making it difficult to assess whether and how built environment factors exert consistent or divergent effects on crime and perceived safety, thereby constraining the practical relevance of research for urban design and safety governance. Fourth, few studies have examined the alignment between subjective perceptions and objective risks from the perspective of coupling and coordination across different areas, resulting in an incomplete understanding of spatial safety as an integrated phenomenon.

Accordingly, this study has four objectives: (1) to examine differences in residents' safety perception of the same urban spaces between daytime and nighttime and

characterize their spatial clustering patterns; (2) to evaluate the spatial correspondence between safety perception and daytime and nighttime crime patterns and identify areas in which the two exhibit local mismatches; (3) to examine the differentiated associations of activity density, governance facilities, streetscape characteristics, built-environment conditions, and other contextual factors with daytime and nighttime crime rates, and to formally test potential indirect pathways through safety perception; and (4) to assess the coupling coordination between safety perception and crime rates and characterize their spatial matching states across different areas.

To address these objectives, we integrate adjudicated and publicly disclosed criminal cases, street-view imagery, generative image transformation, questionnaire-based safety perception ratings, and multiple urban environmental indicators within a unified analytical framework. First, a CycleGAN-based D2N model is used to construct corresponding nighttime streetscapes, while survey ratings from Shanghai residents provide locally grounded safety perception measures. Second, GCNNWR is employed to examine spatial heterogeneity in the associations between environmental factors and crime rates, while a bootstrap-based mediation framework is used to evaluate potential indirect pathways through safety perception. Third, we calculate the coupling coordination degree between daytime and nighttime safety perception and crime rates to identify differences in coordination states across administrative districts.

This study provides empirical evidence to support fine grained governance aimed at enhancing urban perceived safety, informs the optimization of nighttime environments and the improvement of residents' safety experiences, and offers policy relevant insights for promoting socially equitable and safe urban development in high-density cities.

2. Data and methodology

2.1 Study area

This study examines day and night crime in Shanghai, China (Fig. 1a and 1b). As one of China' s leading economic centers, Shanghai has one of the largest urban economies in the country in terms of total gross domestic product (GDP) and has ranked first in the China Nighttime Economy Index for five consecutive years (Government, 2025). However, the high intensity economic operation and high-density spatial development are accompanied by social governance pressures. From 2000 to 2019, the total number of criminal cases in Shanghai exceeded 30,000, making it one of the cities with the highest crime counts nationwide (Zhang et al., 2025). Within this rapidly developing urban system, growing economic and population vitality has intensified residents' demands for safety and order.

In this context, this study selects seven old urban districts in central Shanghai:

Yangpu, Hongkou, Jingan, Putuo, Changning, Xuhui and Huangpu (Fig. 1b). The basic spatial unit of analysis was the community, defined according to the community-level boundaries of the Seventh National Population Census of China in 2020. Fig. 1c further presents representative examples of selected crime types and the SVI corresponding to their locations. This study will provide insights and references for optimizing urban street environment design, enhancing residents' safety perception, and improving day and night governance strategies.

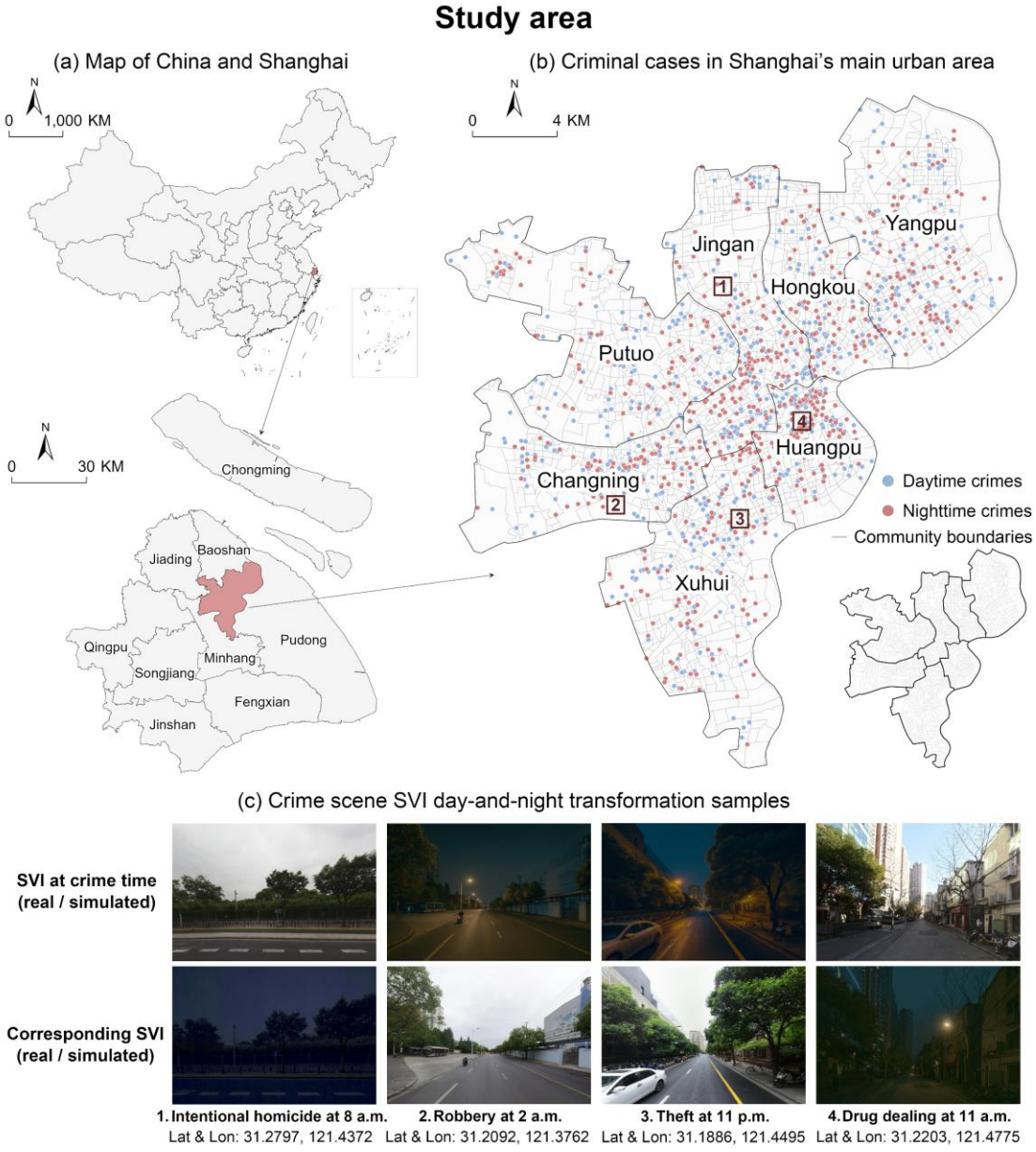


Fig. 1 Study area and distribution of daytime and nighttime crimes in central Shanghai

2.2 Research framework

To clearly illustrate the relationships among day-night safety perceptions, street level visual elements, the built environment, and crime patterns, and to present the overall

analytical process of the study, a research framework was developed (Fig. 2). A more detailed version of the research framework is provided in section 1 of the supplementary information.

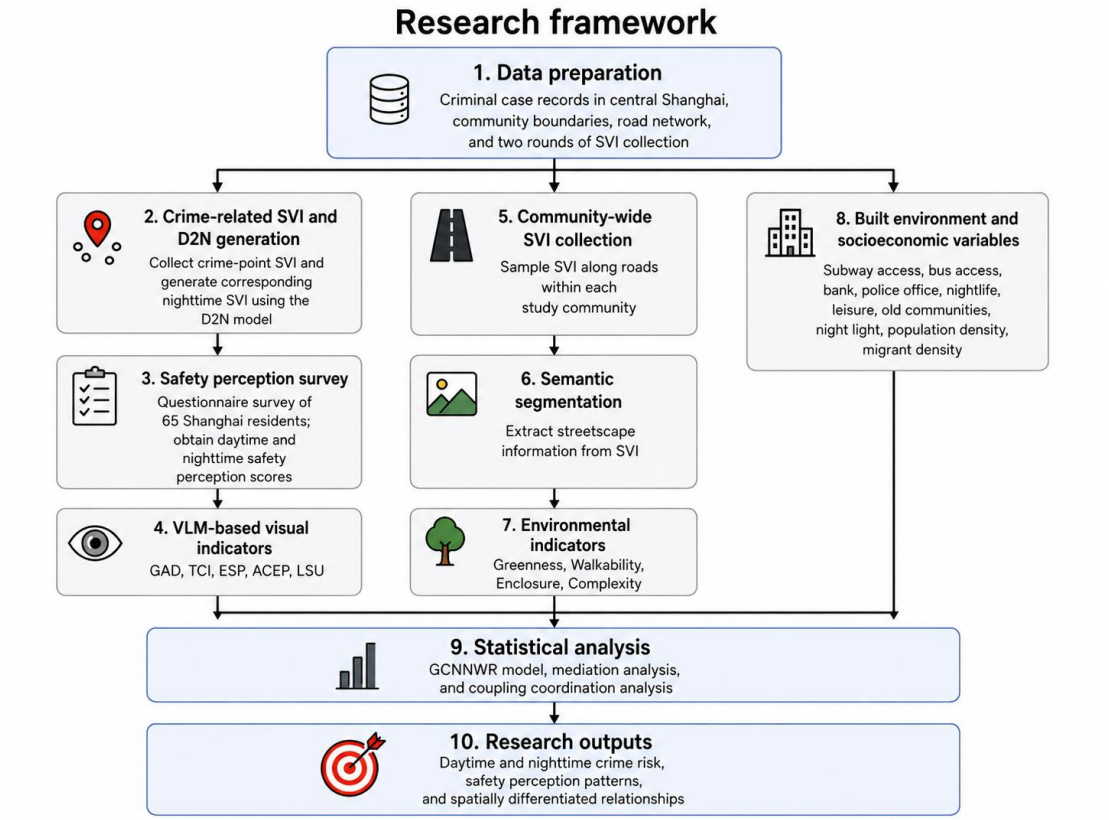


Fig. 2 Research framework for day-night streetscape perception and crime modelling

2.3 Data Sources and Processing

2.3.1 Crime rate as dependent variables

As the principal national-level court judgment disclosure platform in China, the China Judgements Online Platform (https://wenshu.court.gov.cn/) contains a large collection of publicly available judicial judgment documents and provides source for identifying adjudicated criminal cases (Zhang et al., 2025). We utilized web scraping techniques to obtain adjudicated and publicly disclosed criminal case records from Shanghai's central urban area during 2017 to 2019 (including robbery, theft, intentional injury, and others). Subsequently, we employed the Baidu Map API to geocode location descriptions in case texts, converting them to the standard WGS84 coordinate system, and conducted cross validation and calibration through Google Maps to correct deviations arising from different coordinate systems.

After excluding invalid cases and those with missing information, we manually identified and verified the occurrence time of each case, classifying cases occurring between 6:00 and 20:00 as daytime crimes and those occurring between 20:01 and 5:59 as nighttime crimes. Following multiple rounds of data cleaning and quality control,

we ultimately obtained 1,800 daytime crime cases and 1,064 nighttime crime cases. Finally, we used ArcGIS Pro 3.3 to aggregate day and night crime data to different census communities and calculated crime rate per thousand based on permanent resident population for subsequent analysis.

2.3.2 Safety perception factors as independent variables

We conducted two separate rounds of SVI collection. The present round was conducted to obtain daytime and nighttime crime-related SVI, which were subsequently used to derive residents' subjective safety perception scores.

Fig. 3 illustrates the process of collecting subjective safety perception data. First, daytime SVI were collected at locations where daytime and nighttime crimes occurred. The corresponding nighttime SVI were then generated using the D2N model. Baidu Maps (https://map.baidu.com/) is one of the digital map platforms with the widest coverage and highest update frequency in China(Yu et al., 2025). When constructing the sample, we deduplicated multiple cases at the same coordinates, ultimately obtaining 1,766 independent crime points in total, including 1,047 daytime and 719 nighttime crime points. Subsequently, we requested corresponding SVI through the Baidu Maps Open Platform API, with shooting parameters uniformly set as follows: viewing angle parallel to the road centerline, horizontal field of view at 90 degrees, pitch angle at 0 degrees, and resolution maintained at 640 by 400 pixels. A total of 1,766 SVI were ultimately obtained, all captured during 2017 to 2019 to ensure temporal consistency.

Second, a D2N model was trained to simulate nighttime crime SVI. We conducted training with reference to samples provided by Ye et al. (2025) and Z. Liu et al. (2024), and trained the D2N model based on CycleGAN. Specifically, we divided 908 sets of SVI into a training set (851 pairs) and a test set (57 pairs, approximately 6%), which included 304 pairs of samples from Shanghai's central urban area to enhance evaluation independence. Subsequently, the training set was input into CycleGAN to complete the D2N model training. The generated results from the model encompassed two categories for subsequent subjective safety perception research: (1) authentic daytime SVI corresponding to daytime crime events and their generated simulated nighttime counterparts; (2) simulated nighttime SVI corresponding to nighttime crime events and their authentic counterparts.

We conducted a direct visual comparison using five representative street locations with available daytime and authentic nighttime SVI (Fig. S2). For each location, the daytime, authentic nighttime, and D2N-generated nighttime images were compared side by side. The generated images generally preserved stable physical characteristics, including road geometry, building configuration, vegetation distribution, street boundaries, and enclosure structure, while reproducing key nighttime visual features

such as reduced ambient illumination, darker vegetation and sky, increased contrast, and localized artificial-light effects. Overall, the generated nighttime scenes were broadly consistent with the corresponding authentic nighttime SVI.

Third, a resident subjective safety perception survey was conducted. We recruited 65 permanent residents of Shanghai and distributed questionnaires through the Tencent Questionnaire platform (https://wj.qq.com/). The survey procedure included participant information collection (age, years of residence), Ishihara color blindness test screening, SVI rating, and data verification. During the formal rating phase, the questionnaire presented SVI one image per page, randomly displaying daytime and nighttime images, with respondents required to observe for no less than five seconds before answering. Ratings adopted a nine-point scale, with each image corresponding to six questions that respectively measured six core subjective perception indicators to capture multidimensional safety perception differences. Additionally, to enhance data consistency and reliability, ten experts in urban planning reviewed the ratings. SVI samples with incomplete ratings or implausible scoring results were excluded according to predefined criteria. After quality control, 1,751 valid SVI samples remained, yielding 10,506 rating records. Detailed robustness and sensitivity analyses of the safety perception ratings are provided in section S3 of the supplementary information.

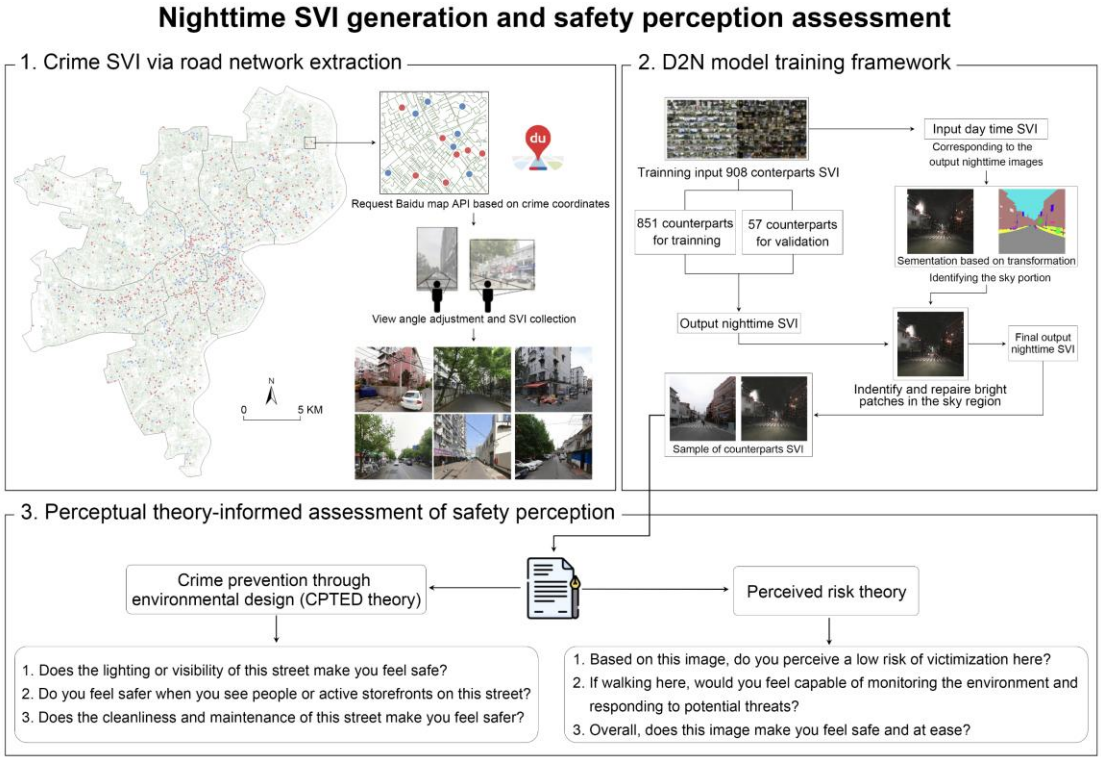


Fig. 3 Nighttime SVI generation using the D2N model and collection of subjective safety perception via questionnaires

2.3.3 Environmental factors as independent variables

The second round of SVI collection was conducted to quantify environmental factors across the study areas.

We first obtained the complete road network of Shanghai from Baidu Maps and clipped it according to the study area and community boundaries. The road network was then standardized in ArcGIS Pro 3.3 through procedures including road merging and node optimization. Based on the processed road network, SVI sampling points were generated at fixed 50-meter intervals along all roads within each study community. Corresponding 360° panoramic street-view images were retrieved through the Baidu Maps Open Platform API. To ensure temporal consistency and scene comparability, all SVI were collected from imagery captured between 2017 and 2019. After removing duplicate and low-quality samples, a total of 68,543 valid SVI retained.

Fig. 4 illustrates the workflow for semantic segmentation and environmental feature extraction. We employed a Mask2Former model pretrained on the ADE20K dataset to perform semantic segmentation of the SVI. ADE20K contains 27,574 annotated images covering 150 scene categories, supporting the identification of diverse environmental elements in streetscapes. Based on the segmentation results and following Hamim and Ukkusuri (2024) and Zhou et al. (2024), we derived four streetscape dimensions: greenness, walkability, enclosure, and complexity. The corresponding indicators were averaged across all valid SVI within each community to construct community-level environmental variables. The definitions, components, and calculation methods of these indicators are presented in Table 1.

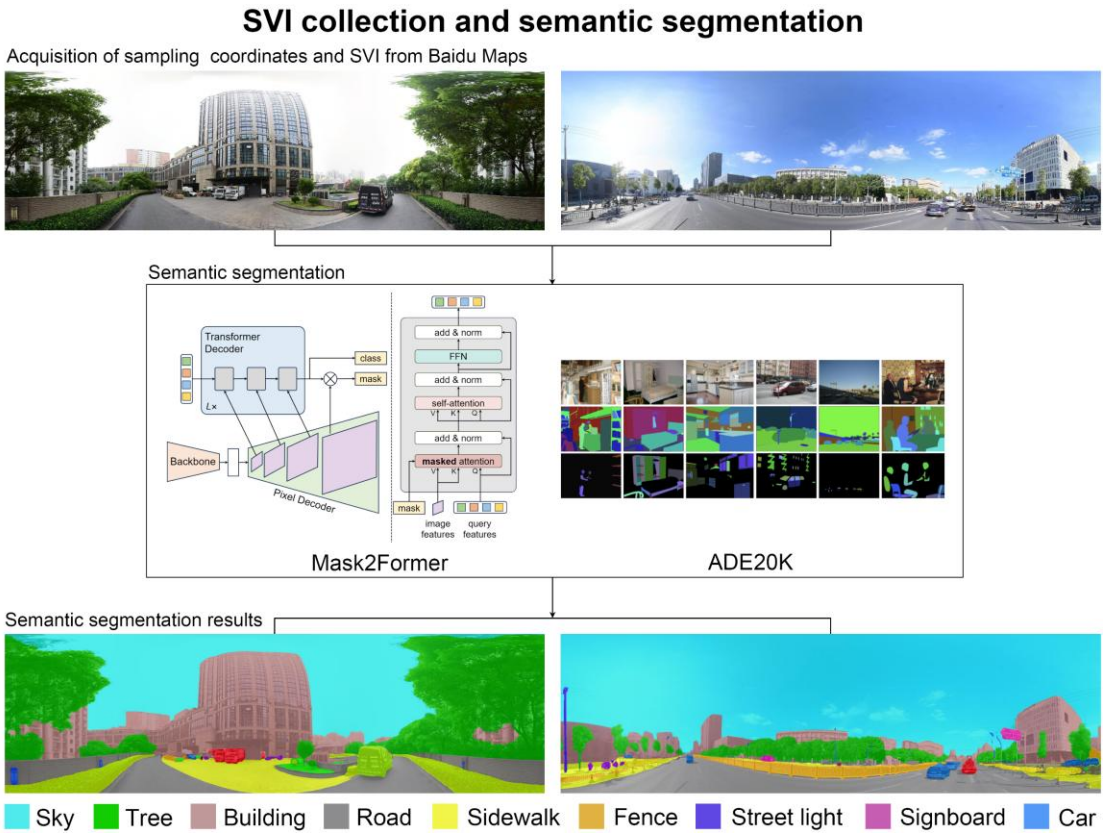


Fig. 4 SVI collection and semantic segmentation process

Table 1 Definitions for environmental factors from four perceptual qualities

Perception	Definition	Examples	Objective formulas (based on referable and operational definitions)
Greenness	Greenness refers to the amount of natural vegetation within a space, including trees, grass, and shrubs(Suzuki et al., 2023; S. Wang et al., 2026).	High greenness typically features broad, tree-lined streets or continuous greenbelts.	$Greens_i = VI_{tree} + VI_{grass} + VI_{plant}$ (Woo et al., 2024)
Walkability	Walkability refers to how surrounding visual features contribute to walking comfort, and how they shape the pedestrian-friendly qualities of elements such as sidewalks and barriers(Wang & Rasouli,	High walkability typically features continuous sidewalks and safe crossing points, enhancing pedestrian convenience and safety.	$Walkb_i = \frac{VI_{sidewlk}+VI_{fence}}{VI_{road}}$ (Shin & Woo, 2024)

	2022).		
Enclosure	Enclosure refers to the degree to which streets and other public spaces are visually defined or framed by buildings, fences, walls, trees, and other vertical elements(Ewing & Handy, 2009; Pradana et al., 2025).	High enclosure indicates that the street is strongly defined by vertical elements, creating a more focused space with a clearer pedestrian scale.	$Encls_i = \frac{VI_{bldg}+VI_{tree}+VI_{wall}}{VI_{road}+VI_{sidewlk}+VI_{earth}+VI_{grass}}$ (Qiu et al., 2023)
Complexity	Complexity refers to the visual richness produced by diverse street elements, reflected in the share of detailed, engaging components relative to basic features such as buildings and roads(Ewing & Handy, 2009).	High complexity refers to streets that, compared with simpler surfaces, feature more signage, decorative lighting, and varied edge treatments.	$Cmplx_i = \frac{VI_{person}+VI_{signb}+VI_{fence}+VI_{strlgt}+VI_{tree}+VI_{Win}}{VI_{bldg}+VI_{road}}$ (Qiu et al., 2023)

2.3.4 Vision large model (VLM) factors as independent variables

To characterize the effects of SVI environments on day and night crime rate, we constructed five visual dimension indicators based on SVI as independent variables (Table 2). Specifically, we invoked the ChatGPT 5 VLM API to perform automated interpretation of SVI extracted around each crime point, and strictly following the operationalized definitions in Table 2, assigned scores ranging from 1 to 9 for each of the five dimensions, while outputting brief interpretation rationales to enhance interpretability and facilitate quality inspection. In total, VLM scores for five perceptual dimensions were obtained from 1,757 crime-related SVI images and used in the subsequent regression analyses (Detailed operational procedures for scoring, output generation, and quality control are provided in Section 2 of the Supplementary Information).

Table 2 Operational definitions of five VLM derived SVI dimensions

Dimension	Definition
Guardianship and Activity Density (GAD)	Captures the potential for street-level natural surveillance, indicated by the density of visible routine users (e.g., pedestrians,

	cyclists) and their activity intensity.
Territoriality and Caretaking Index (TCI)	Measures the extent to which a space is cared for and territorially claimed, operationalized as the balance between cues of order (e.g., cleanliness) and cues of disorder (e.g., litter accumulation, graffiti).
Eye Surveillance Potential (ESP)	Represents passive surveillance potential from the built frontage, reflected in street-facing openings such as doors, windows, and balconies.
Access Control and Edge Perimeter Controllability (ACEP)	Assesses the controllability of access points and edges, based on the proportion of controlled entrances (e.g., access gates, bollards, fences) relative to uncontrolled passages (e.g., alleys, gaps in fences), while accounting for blind-spot risk.
Lighting Sufficiency and Uniformity (LSU)	Reflects overall nighttime lighting quality, jointly evaluating lighting coverage, roadway brightness, and illumination uniformity.

The five VLM-derived variables were intentionally constructed from crime-related SVI rather than from the systematic road-network sample because they were designed to characterize micro-scale visual conditions surrounding observed crime locations. This sampling support differs from that used for the four community-wide streetscape indicators in Section 2.3.3, which were derived from systematic 50-m sampling along the entire road network to represent the general environmental context of each community.

For subsequent community-level analyses, the VLM scores of all valid crime-related SVI within each community were aggregated to obtain community-level mean values for GAD, TCI, ESP, ACEP, and LSU. Therefore, although the two SVI datasets were collected using different sampling strategies, they represent two complementary spatial supports: community-wide environmental context and crime-location-specific visual conditions. The former was used to characterize general streetscape exposure, whereas the latter was used to capture visual cues directly associated with crime settings and perceived safety. The use of crime-related SVI for the VLM indicators also ensured consistency with the perceived-safety measures used in the mediation analysis, because both were derived from the same set of crime-related street environments before aggregation to the community level.

2.3.5 Built environment factors as independent variables

We first obtained point of interest (POI) data for Shanghai in 2019 through Baidu Maps and filtered them according to the study area to characterize built environment distribution. To more accurately explore the relationship between crime and built environment, we split and merged the original 14 major POI categories. Specifically,

we split categories such as "sports and leisure" and "government agencies and social organizations," and extracted "police office" and "bank" POIs through keyword matching. We merged keywords including "KTV," "bar," "nightclub," and "internet cafe" into the "nightlife" category to reflect the concentration of venues with high pedestrian flows during nighttime hours. Additionally, by merging subcategories such as "shopping services" and "catering services," we constructed the "leisure" category representing consumption oriented built environments.

In addition to POI data, we also obtained residential community information from Anjuke (https://shanghai.anjuke.com/) through web scraping. According to national policy standards, we screened residential areas constructed before 2000 and defined them as the "old communities" category(S. Wang et al., 2026), to capture potentially structurally vulnerable areas within urban spaces. Ultimately, we focused on five categories of built environment factors: police office, bank, nightlife, leisure, and old communities, and calculated their respective densities across different communities as built environment factors.

2.3.6 Socioeconomic factors as control variables

To reduce potential bias in model predictions, we included demographic, transportation accessibility, and socioeconomic characteristics as control variables, which have been widely used in crime research(Maia et al., 2025; Snowden et al., 2025). Demographic data were derived from the Seventh National Population Census in 2020, which is temporally closest to the crime records in this study. We calculated total population density and migrant population density based on community level data to reflect differences in population size and population structure. Transportation accessibility was based on subway station and bus station POIs, using ArcGIS Pro 3.3 combined with road network distances to calculate the distance from each crime point to subway stations and bus stations in the study area, thereby measuring the degree of public transportation accessibility.

Socioeconomic status was proxied by NPP VIIRS nighttime light (NTL) as a surrogate indicator of economic vitality(Sarif & Roy, 2024). Since NTL is highly sensitive to brightness and susceptible to interference from non urban light sources such as wildfires, we set a peak brightness ceiling during preprocessing to attenuate the influence of outliers. Subsequently, we utilized the zonal statistics tool in ArcGIS Pro 3.3 to calculate the mean nighttime light intensity for each community in 2019.

2.4 Model construction

The two analytical stages were designed to address different but sequential research questions. First, GCNNWR was used as a broad spatial analysis to identify how visual, built-environment, and socioeconomic characteristics were associated with daytime

and nighttime crime rates and to capture spatial heterogeneity in these relationships. Second, the mediation analysis focused specifically on the potential perceptual mechanism linking visible street-level environmental cues to crime risk through safety perception.

The five VLM-derived variables were selected as focal variables in the mediation analysis because they represent visual characteristics that can be directly perceived from the street environment and are theoretically related to guardianship, territoriality, surveillance, access control, and lighting. These characteristics may therefore influence crime not only directly, but also indirectly by shaping residents' safety perception. In contrast, broader contextual variables such as population density, migrant density, transportation accessibility, and nighttime light were treated as background covariates rather than mediation candidates because their relationships with crime do not necessarily operate through visual safety perception.

2.4.1 Graph convolutional neural network weighted regression model

Geographically weighted regression (GWR) models often face limitations in accurately capturing spatial non-stationarity, as spatial weight calculations require pre-specifying kernel functions and their bandwidths(Xu et al., 2025). Kernel functions themselves exhibit inherent rigidity and lack flexibility in form. In contrast, Convolutional Neural Network (CNN) models excel at extracting spatial features and can flexibly customize their structure to accommodate specific attributes of sample data. Therefore, this study combines CNN with Ordinary Least Squares Regression (OLS) to develop the GCNNWR model for estimating spatial non-stationarity. The GWR model incorporates the spatial relationship between regression coefficients and geographic locations, which can be expressed as follows(1):

$$y_i = \beta_0(u_i, v_i) + \sum_k \beta_k(u_i, v_i) x_{ik} + \varepsilon_i \tag{1}$$

Where: y_i represents the dependent variable, $\beta_0(u_i, v_i)$ denotes the constant term. $\beta_0(u_i, v_i)$ denotes the regression coefficient for the k-th explanatory variable. x_{ik} denotes the k-th feature of the i-th observation, ε_i is the random error term.

The weighted least square method (WLS) is commonly used to evaluate GWR models and can be expressed as follows(2)(3)(4):

$$\hat{\beta}(u_i, v_i) = \left(X^{\mathrm{T}} W(u_i, v_i) X\right)^{-1} X^{\mathrm{T}} W(u_i, v_i) y \tag{2}$$

$$\hat{y}(u_i, v_i) = x_i^T \hat{\beta}(u_i, v_i) \tag{3}$$

$$W(u_i, v_i) = f_{\text{kernel}}(D_i) \tag{4}$$

Where: $\hat{\beta}(u_i, v_i)$ represents the vector of estimated parameters. $W(u_i, v_i)$denotes the weighting matrix for the i-th observation, D_i is the distance matrix. f_{kernel} denotes the kernel function. X denotes the feature matrix, x_{ik} and y denote the dependent variable vector.

The GCNNWR model aims to leverage the multidimensional feature learning capability of CNNs to replace the estimation process of the weight matrix $W(u_i, v_i)$ in traditional GWR models. Spatial non-stationarity describes spatial variations in the spatial domain's mean stationarity relationship, which is typically characterized by OLR models(B. Liu et al., 2024). Therefore, spatial non-stationarity can be understood as the variation of the mean stationarity relationship with spatial location, expressed as (5):

$$y(u_i, v_i) = w_0(u_i, v_i)\beta_0 + \sum_p w_k(u_i, v_i)\beta_k \; x_k(u_i, v_i) + \varepsilon_i \tag{5}$$

Where: β_k and β_0 denote the k-th coefficient and the constant term in the OLR model, $w_k(u_i, v_i)$ and $w_0(u_i, v_i)$ represent the geographic weight and the constant term for the k-th explanatory variable, respectively.

Additionally, $\hat{y}(u_i, v_i)$ represents the estimated value, which can be expressed as (6):

$$\hat{y}(u_i, v_i) = x_i^T W(u_i, v_i)(X^T X)^{-1} X^T y = x_i^T W(u_i, v_i)\widehat{\beta_L} \tag{6}$$

Where: $W(u_i, v_i)$ is the global geographic weight matrix for the i-th observation computed by the CNN model, expressed as (7)(8):

$$W(u_i, v_i) = CNN\left(\overline{D}_i\right) \tag{7}$$

$$\overline{D}_i = \begin{bmatrix} d_{i-11} & \cdots & d_{i-1n} \\ \vdots & \ddots & \vdots \\ d_{i-m1} & \cdots & d_{i-mn} \end{bmatrix} \tag{8}$$

Where: $\overline{D}_i$ represents the distance matrix of global spatial proximity between all grids and the i-th observation value. n and m denote the total number of grids. CNN denotes the function that calculates the weight matrix using a stacked CNN model, whose convolution process can be expressed as (9):

$$g^{r+1} = \mathit{ReLU}(g^r \cdot M^{r+1} + b^{r+1}) \tag{9}$$

Where: g^r and g^{r+1} are the output of r-th and $(r+1)$-th layers. M^{r+1} is the first layer of matrix $(r+1)$, b^{r+1} is the bias vector.

Model performance comparisons are provided in section 3 of the supplementary information (Tables S4-S5).

2.4.2 Bootstrap-based mediation analysis of safety perception

To formally examine whether safety perception serves as an indirect pathway linking the VLM-derived environmental characteristics to crime risk, we conducted a regression-based mediation analysis. We followed the product-of-coefficients and bootstrap approach developed by Preacher and Hayes (2008) to directly estimate and test indirect effects.

The five VLM-derived indicators, GAD, TCI, ESP, ACEP, and LSU, were specified simultaneously as the focal explanatory variables, with safety perception as the mediator and crime rate as the outcome variable. Safety perception was derived from the questionnaire survey and operationalized as the overall mean perception score calculated from the questionnaire responses, providing an aggregate measure of respondents' perceived safety. Night light, migrant density, population density, subway access, and bus access were included as covariates. To enable direct comparison between temporal contexts, the same mediation specification was estimated separately for daytime and nighttime crime.

First, the mediator model estimated the associations between the five VLM indicators and safety perception (10):

$$M_i = \alpha + \sum_{j=1}^{5} a_j X_{ji} + \gamma^T C_i + \varepsilon_{Mi} \tag{10}$$

Where: M_i represents the safety perception score for spatial unit i, X_{ji} represents GAD, TCI, ESP, ACEP, and LSU, and C_i denotes the set of covariates. The coefficient a_j represents path a, namely the association between each VLM indicator and safety perception after accounting for the remaining VLM indicators and covariates.

Second, the outcome model incorporated both the five VLM indicators and safety perception (11):

$$Y_i = \beta + \sum_{j=1}^{5} c'_j X_{ji} + bM_i + \delta^T C_i + \varepsilon_{Yi} \tag{11}$$

Where: Y_i represents the daytime or nighttime crime rate. The coefficient b represents path b, namely the association between safety perception and crime rate conditional on the five VLM indicators and covariates. The coefficient c'_j represents the direct effect of each VLM indicator on crime rate after accounting for safety perception.

Third, the total association between each VLM indicator and crime rate was estimated without including safety perception (12):

$$Y_i = \mu + \sum_{j=1}^{5} c_j X_{ji} + \theta^T C_i + \varepsilon_{Yi} \tag{12}$$

Where: c_j represents path c, or the total effect of each VLM indicator on crime rate before accounting for safety perception.

The indirect effect of each VLM indicator through safety perception was calculated using the product-of-coefficients approach (13):

$$IE_j = a_j \times b \tag{13}$$

Where: $a_j \times b$ represents the indirect pathway from a given VLM indicator to crime rate through safety perception.

All continuous variables were standardized prior to estimation, and HC3 heteroskedasticity-robust standard errors were used for individual regression coefficients. Indirect effects were evaluated using 20,000 nonparametric bootstrap resamples, from which bias-corrected and accelerated (BCa) 95% confidence intervals were obtained. An indirect effect was considered statistically supported when its BCa 95% CI did not include zero.

2.4.3 Coupling coordination degree model

To further identify the degree of coordination between safety perception and crime conditions across communities, this study employs the coupling coordination degree model. This approach not only characterizes the strength of the interaction between two systems but also evaluates whether their relationship is associated with a relatively balanced overall state. Specifically, the coupling degree C measures the degree of interaction between the two systems, the comprehensive development index T represents their overall status, and the coupling coordination degree D integrates both dimensions to assess the level of coordination between them (Li et al., 2012). In this study, the model is used to identify the spatial correspondence between safety perception and urban public safety, thereby complementing the preceding analyses of their spatial distributions and statistical associations.

Because safety perception and recorded crime rate have opposite directional meanings, the two variables were first normalized. Safety perception was positively normalized, such that higher values indicate higher levels of safety perception, whereas recorded crime rate was inversely normalized, such that higher values indicate lower crime risk and thus a higher level of public safety. The normalized indices are denoted as u_1 *and* u_2, respectively, both ranging from 0 to 1. The coupling degree is calculated as follows (14):

$$C = 2\sqrt{\frac{u_1 u_2}{(u_1+u_2)^2}} \tag{14}$$

Where: C denotes the coupling degree, ranging from 0 to 1. A higher value of C indicates stronger interaction or synchronization between the two systems. However,

a high coupling degree does not necessarily imply that both systems are at relatively favorable levels. Therefore, the comprehensive development index is further calculated as (15):

$$T = \alpha u_1 + \beta u_2 \tag{15}$$

Where: T denotes the comprehensive development index, α and β represent the weights assigned to safety perception and public safety, respectively. Because this study focuses on their relative coordination and has no a priori basis for assigning greater importance to either subsystem, equal weights are assigned, with α = β = 0.5.

Based on C and T, the coupling coordination degree is calculated as (16):

$$D = \sqrt{C \times T} \tag{16}$$

Where: D denotes the coupling coordination degree, ranging from 0 to 1. A higher value of D indicates a higher degree of coordination between safety perception and lower crime risk at the city level, whereas a lower value indicates greater discordance between the two. This measure therefore helps identify cross-city differences that cannot be fully captured by examining safety perception or crime rate independently.

3. Results

3.1 Spatial distribution of day and night crime rate and subjective safety perception

Fig. 5a and 5b present the spatial distribution of daytime and nighttime crime rate in Shanghai's central urban area. Overall, nighttime crime rate are slightly lower than daytime rates, exhibiting a declining trend associated with reduced daylight hours(Domínguez & Asahi, 2023). Specifically, day and night crime hotspots demonstrate high spatial overlap, primarily concentrated in the central, southwestern, and northeastern areas. These regions are characterized by intensive commercial activities and concentrated residential populations, thereby presenting higher probabilities of criminal offenses(Jiang et al., 2024). Fig. 5c further illustrates crime rate differences across administrative districts. Among them, Huangpu District exhibits the highest crime rate during both daytime and nighttime periods, which may be attributed to its inclusion of core attractions such as the Bund, where tourists and transient populations are highly concentrated. In contrast, Putuo, Changning, Xuhui, and Yangpu Districts maintain relatively lower overall levels. In general, although overall nighttime crime rate show a slight decline, day and night crime patterns demonstrate strong spatial consistency.

To examine the spatial mismatch between crime and safety perception, we mapped the spatial distribution of safety perception for daytime and nighttime crime scene SVI based on questionnaire ratings (Fig. 5d and 5e). Overall, nighttime safety

perception scores are generally lower than daytime scores, indicating that nighttime visual environments diminish residents' safety perception on the whole, consistent with findings from existing studies(Ye et al., 2025). Specifically, the mean daytime safety perception score is 6.29, with low values primarily distributed in the central western and northeastern areas, partially overlapping with high crime zones; peripheral areas (such as the south and west) exhibit higher scores, yet some central areas simultaneously present mismatch phenomena characterized by both higher safety perception and higher crime rate.

The mean nighttime safety perception score is 6.02 (Fig. 5e), with low values demonstrating stronger continuity and clustering in the central, northeastern, and northwestern areas, while the southern and western regions maintain relatively higher overall scores. Certain northeastern and northwestern areas exhibit mismatch phenomena with nighttime crime rate. Fig. 5f further illustrates safety perception differences across administrative districts. Similarly, Huangpu District exhibits relatively more low values in both daytime and nighttime SVI categories, corresponding to the high crime rate shown in Fig. 5c. In comparison, Jingan and Xuhui Districts demonstrate relatively higher overall safety perception scores.

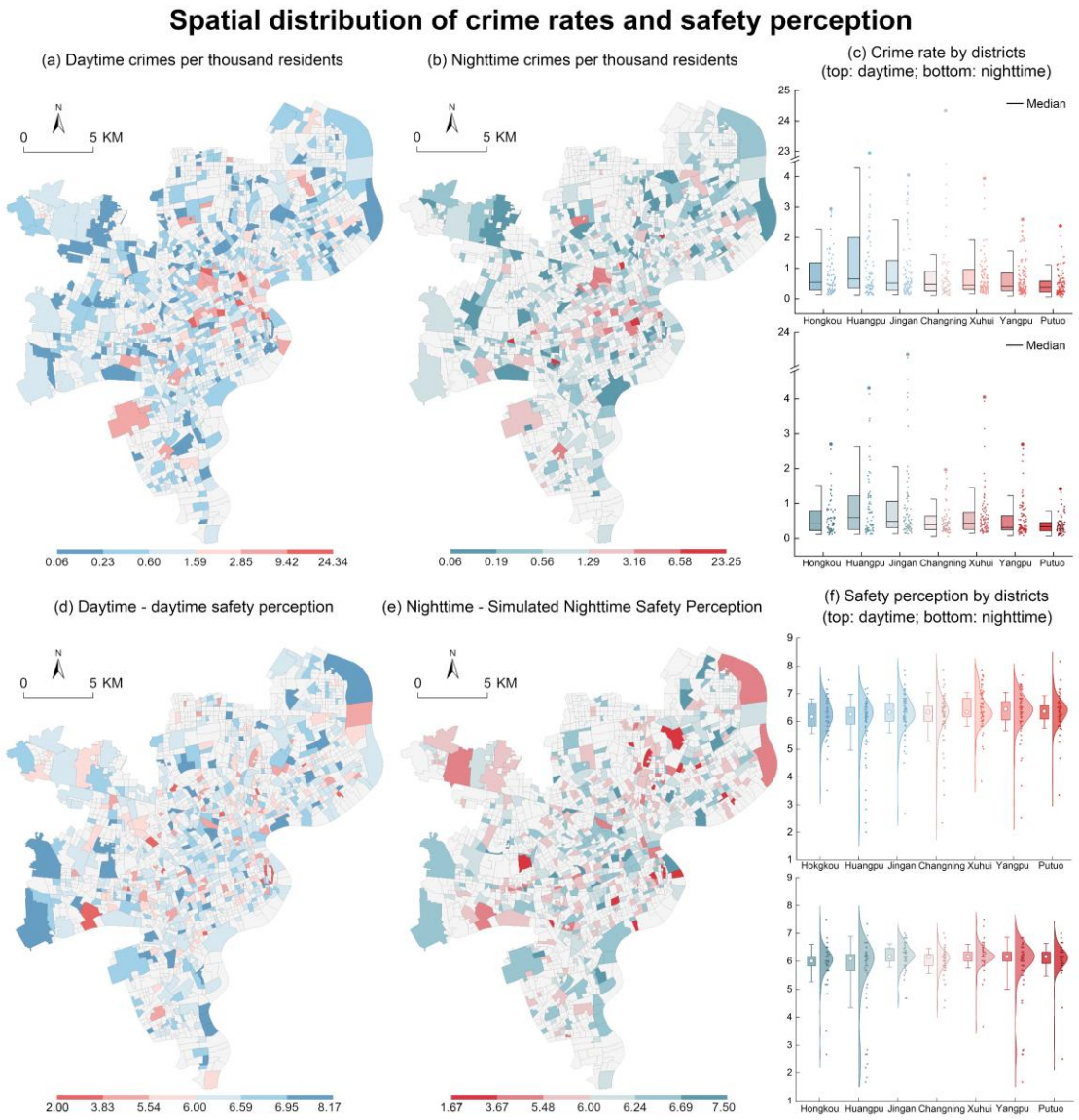


Fig. 5 Spatial distribution of crime rate and safety perception across daytime and nighttime conditions

3.2 Effects of potential factors on day and night crime rate

To examine the spatially varying associations between potential factors and community crime rates across daytime and nighttime periods, we employed the GCNNWR model to capture local heterogeneity (Fig. 6). As shown in Fig. 6a, daytime crime rate were positively associated with GAD and leisure facilities, suggesting that areas with greater daytime activity and leisure concentration may experience higher crime exposure due to more frequent interpersonal interactions. In contrast, migrant density and population density were negatively associated with crime rate, while police office showed a clear negative relationship, indicating a potential deterrent role of formal guardianship during the daytime.

Nighttime patterns differed substantially (Fig. 6b). Leisure, night light, nightlife, and

old communities were positively associated with crime rates, whereas the negative association with police office became weaker. ESP also showed a positive association, suggesting that passive visual exposure from building facades may not necessarily translate into effective surveillance at night. Meanwhile, the association of GAD weakened, highlighting temporal variation in the role of activity density. Among streetscape factors, walkability was positively associated with nighttime crime rates, whereas enclosure, complexity, and greenness showed predominantly negative associations.

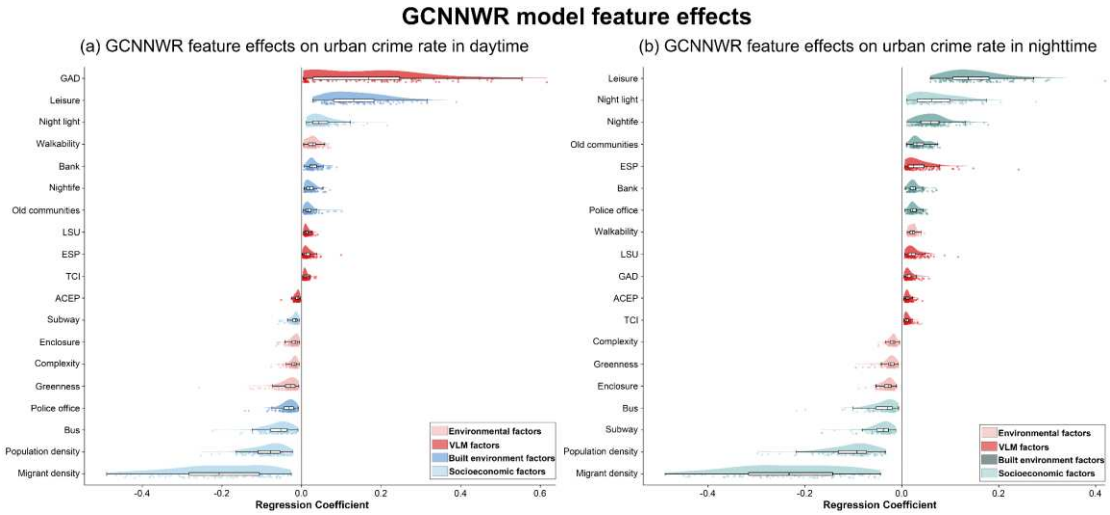


Fig. 6 GCNNWR model feature effects on daytime and nighttime urban crime rate

3.3 Nonlinear relationships between different safety perception dimensions and day and night crime rate

Fig. 7 illustrates the nonlinear relationships between different safety perception dimensions and crime rate under day and night conditions. Among CPTED related dimensions, natural surveillance (a) and overall sense of safety (f) demonstrate relatively stable effects on day and night crime rate, exhibiting only minor fluctuations, indicating that singular environmental visibility or overall safety evaluations have limited direct regulatory effects on crime. In contrast, social surveillance (b) exhibits an overall upward trend in relation to both daytime and nighttime crime rate, suggesting that increased pedestrian activity on streets corresponds with elevated crime rate. Maintenance and order (c) presents notable day and night differences. When scores fall within the 5 to 6 range, nighttime crime rate decline markedly while daytime crime rate increase; when scores exceed 6, nighttime crime rate conversely rise while daytime rates display unstable fluctuations.

Among perceived risk theory related indicators, perceived control (e) exerts the influence on crime rate. When scores exceed approximately 5.5, both daytime and nighttime crime rate exhibit pronounced fluctuations, with daytime fluctuation

amplitudes substantially greater than those at night, indicating that changes in individuals' subjective assessments of environmental controllability are highly synchronized with crime rate variations. Perceived victimization risk (d) shows gradual increases in both daytime and nighttime crime rate when scores fall below 5.8; when scores surpass this threshold, crime rate display notable fluctuations and tend to stabilize after approximately 6.5. Overall, different perception dimensions exhibit pronounced day and night differentiation across various score intervals, and singular environmental or overall safety indicators cannot comprehensively explain crime variations. The perceived sense of control and victimization risk at the perceptual level hold non negligible importance in characterizing crime fluctuations.

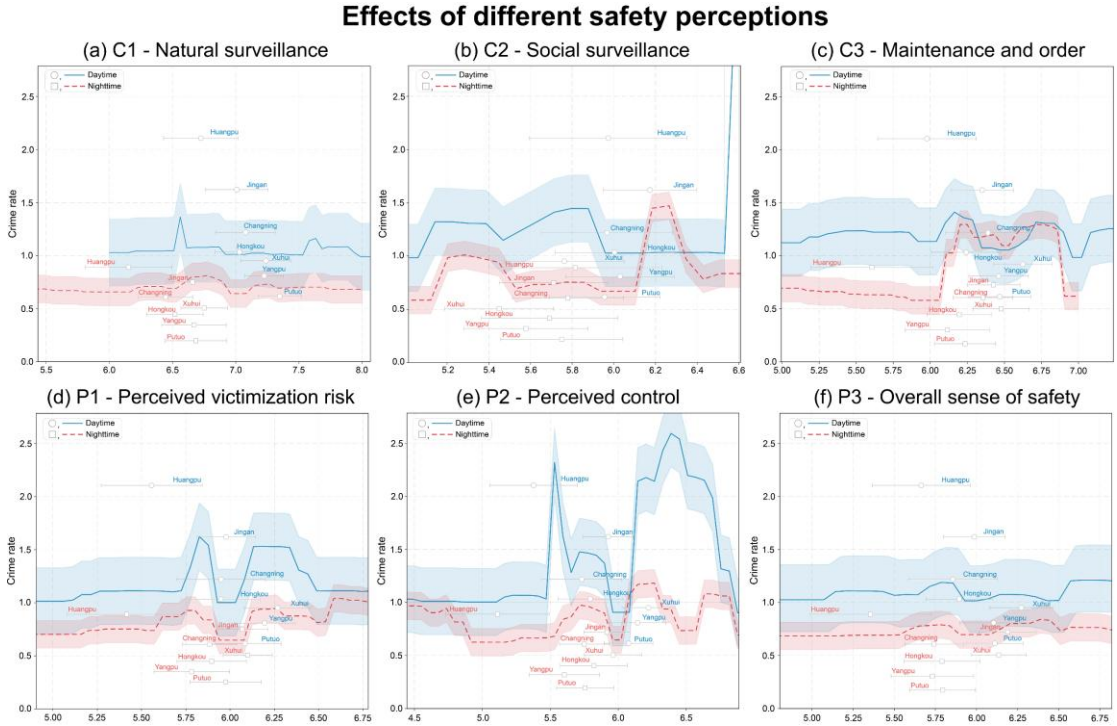


Fig. 7 Effects of different safety perceptions on daytime and nighttime crime rate

3.4 Safety perception as a mediating variable explaining crime rate

The mediation analysis revealed clear day-night differences in the indirect role of safety perception. During the daytime, safety perception showed a weak and non-significant association with crime rate (path b=−0.008, p=0.804). Although TCI was positively associated with safety perception (path a=0.460, p<0.001), none of the five VLM-derived environmental characteristics showed a statistically supported indirect effect on daytime crime, as all bias-corrected and accelerated (BCa) 95% confidence interval included zero.

In contrast, safety perception showed a negative, although individually non-significant, association with nighttime crime rate (path b=−0.094, p=0.089). Both TCI and LSU were positively associated with safety perception, with path-a coefficients of

0.261 and 0.340, respectively (p<0.001 for both). More importantly, their indirect effects on nighttime crime through safety perception were negative and statistically supported. Specifically, the indirect effect was −0.024 for TCI (95% CI: [−0.065,−0.002]) and −0.032 for LSU (95% CI: [−0.078,−0.003]). These results indicate that stronger territoriality and caretaking cues and greater lighting sufficiency and uniformity were associated with higher safety perception, which was in turn associated with lower nighttime crime risk.

Notably, LSU retained a positive direct association with nighttime crime rate after accounting for safety perception (c'=0.115, p<0.05), whereas its indirect effect through safety perception was negative. This opposing pattern indicates a competitive, or inconsistent, mediation structure, suggesting that nighttime lighting may be associated with crime risk through distinct direct and perception-related pathways. Overall, statistically supported indirect pathways through safety perception were observed only under nighttime conditions, particularly for TCI and LSU.

Table 3 Day-night differences in the direct and indirect effects of VLM-derived environmental characteristics on crime rate through perceived safety

Period	Variable	Path a	Path b	Total effect c	Direct effect c'	Indirect effect (ab)	95% CI
	GAD	0.082		0.105	0.106	-0.001	[-0.012, 0.004]
	TCI	0.460***		-0.011	-0.007	-0.003	[-0.032, 0.024]
Daytime	ESP	-0.016	-0.008	-0.020	-0.021	0.000	[-0.005, 0.005]
	ACEP	0.055		-0.006	-0.006	-0.000	[-0.008, 0.003]
	LSU	0.008		0.046	0.046	0.000	[-0.003, 0.007]
	GAD	0.094		-0.013	-0.004	-0.009	[-0.043, 0.004]
	TCI	0.261***		0.012	0.037	**-0.024**	**[-0.065, -0.002]**
Nighttime	ESP	-0.093	-0.094	0.061	0.053	0.009	[-0.004, 0.047]
	ACEP	0.005		-0.028	-0.027	-0.000	[-0.015, 0.010]
	LSU	0.340***		0.083	0.115*	**-0.032**	**[-0.078, -0.003]**

Note: All models controlled for night light, migrant density, population density, subway access, and bus access. * p<0.05; ** p<0.01; *** p<0.001.

3.5 Coupling coordination characteristics of day and night safety perception and crime rate

Finally, we calculated the coupling coordination degree (CCD) between day and night mean safety perception and crime rate to characterize their spatial synergy states (Fig.

8).

Overall, we found that the daytime CCD index (Fig. 8a) is slightly lower than the nighttime index (Fig. 8e), indicating that the matching degree between daytime safety perception and crime rate is generally weaker than that at night. From the perspective of spatial distribution, low daytime CCD values are primarily clustered in the central western and northeastern areas, generally exhibiting discoordinated or nearly discoordinated states. Medium and high values are concentrated in the southern areas and urban peripheral zones, where safety perception and crime rate demonstrate higher synergy (Fig. 8a). Upon further statistical analysis of mean CCD values across administrative districts, we found that Huangpu District exhibits the highest mean CCD value, which is consistent with the characteristics of "high crime rate and low safety perception" presented in the preceding sections, simultaneously reflecting a highly coupled spatial relationship between the two variables (Fig. 8b).

The spatial pattern of nighttime CCD demonstrates pronounced regional segregation. Low value zones are primarily concentrated in the western and eastern areas, while the central, northeastern, and remaining peripheral areas are predominantly characterized by medium to high value distributions (Fig. 8e). Compared with daytime patterns, the high value range of nighttime CCD is more extensive, and the spatial synergy relationship between nighttime safety perception and crime rate is generally more stable. Additionally, the relatively high mean CCD value of Jingan District also corresponds to the crime rate and safety perception characteristics of this district revealed in the preceding sections (Fig. 8f).

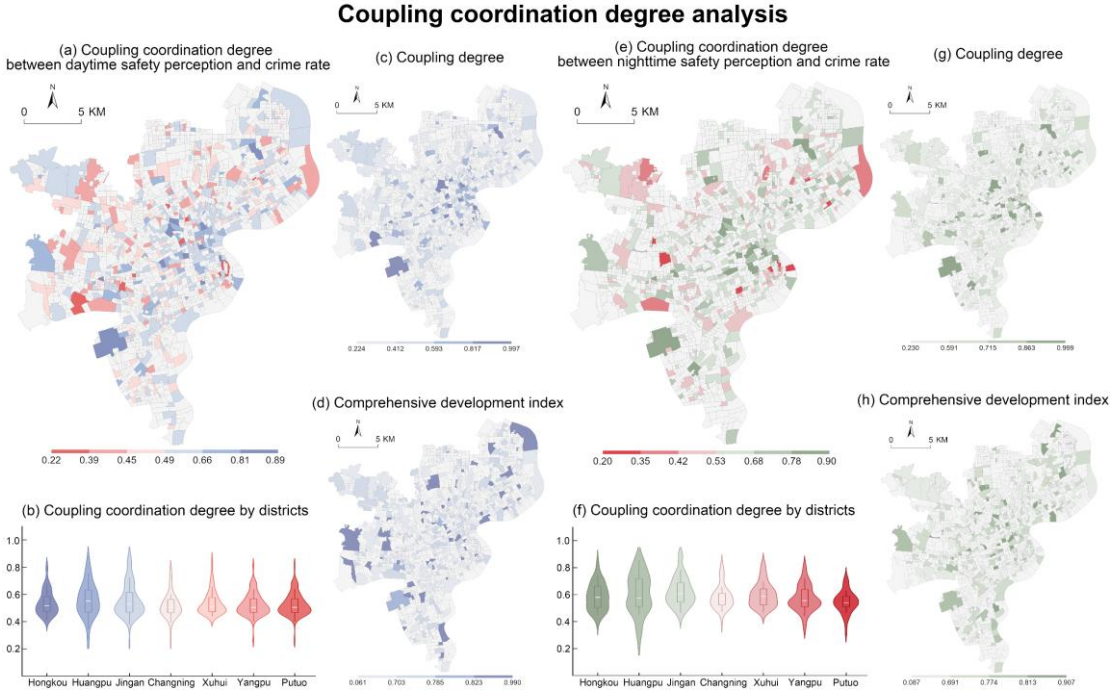


Fig. 8 Coupling coordination degree analysis of safety perception and crime rate across daytime and nighttime conditions

4. Discussion

4.1 Temporal asymmetries in safety perception and crime risk

Our study reveals three key findings that deepen the understanding of the relationship between urban safety perception and crime risk from the day and night temporal dimension.

Our findings suggest that urban safety is not a stable spatial attribute, but a dynamic condition jointly shaped by temporal context, visual environments, and social activity. The greater continuity and clustering of areas with low nighttime safety perception indicate that residents' assessments of crime risk are not determined solely by the spatial distribution of crime events, but are also influenced by environmental visual cues and expectations of spatial controllability (Lorenc et al., 2012; Nasar & Fisher, 1993). This pattern resonates with the environmental-psychological notion of the "geography of fear," whereby fear of crime can develop spatial patterns that are partly independent of crime risk and can subsequently influence everyday spatial behavior through avoidance and withdrawal (Pain, 2000). Thus, the transition from day to night not only alters environmental visibility but may also reshape how residents interpret risk, order, and control in urban space.

The roles of activity intensity and governance facilities also varied across temporal contexts. GAD was positively associated with crime rate, whereas the negative association of police facilities with crime weakened at night. In a high-density city such as Shanghai, intensive street activity may simultaneously increase the number of potential observers and the frequency of encounters, target exposure, and criminal opportunities. Activity density therefore should not be equated directly with effective guardianship. This interpretation is consistent with routine activity theory, which emphasizes the spatiotemporal convergence of suitable targets and capable guardians (Cohen & Felson, 1979). Meanwhile, the weaker nighttime association of police facilities suggests that the presence of static governance infrastructure may not fully substitute for dynamic patrols, visible deterrence, and rapid intervention (Sherman & Weisburd, 1995). These findings indicate that the preventive capacity of both informal and formal guardianship is contingent on temporal context and the actual intensity of surveillance.

More importantly, the role of the visual environment showed a clearer perceptual pathway at night. The mediation analysis identified statistically supported indirect pathways only for TCI and LSU during nighttime: stronger cues of maintenance, order, and territorial care, as well as more sufficient and uniform lighting, were associated with higher safety perception, which in turn was associated with lower nighttime crime risk. This pattern is particularly relevant to Shanghai, where dense commercial, entertainment, and transport activities create nighttime environments characterized by

persistent population flows despite reduced visibility, and where high-activity functions such as leisure facilities are positively associated with nighttime crime. Under these conditions, the maintenance and territorial cues captured by TCI may signal that a space is managed and controllable, which may be associated with greater perceived environmental predictability, consistent with the principles of territoriality and maintenance in CPTED (Jeffery, 1971).

The opposing direct and indirect associations of LSU with nighttime crime suggest that street lighting operates through two distinct mechanisms. The negative indirect pathway can be understood through CPTED and environmental surveillance. More sufficient and uniform lighting improves visibility, reduces visually ambiguous areas, and strengthens perceived environmental controllability, thereby increasing safety perception. In contrast, routine activity theory and rational choice theory help explain the positive direct association (Cornish & Clarke, 2008; Jeffery, 1971). Better illumination may support longer nighttime activities, greater pedestrian presence, and higher concentrations of potential targets. When these increases in activity are not accompanied by sufficient guardianship, improved lighting may coexist with greater crime opportunities rather than directly reducing crime (Welsh & Farrington, 2008).

This dual mechanism is particularly relevant to central Shanghai, where dense mixed land use and concentrated commercial, entertainment, tourism, and transport activities sustain intensive nighttime activity. This interpretation is also consistent with our finding that leisure facilities, nightlife facilities, and nighttime light were positively associated with nighttime crime, while the negative association with police facilities became weaker. Thus, in relatively low-activity residential environments, improving lighting uniformity may mainly reduce visual uncertainty and strengthen perceived control. In highly active commercial and nightlife areas, however, lighting interventions should be combined with visible patrols, crowd management, and other forms of effective guardianship (Hollis-Peel et al., 2011).

4.2 Rethinking crime prevention strategies under high activity density

Our findings have important implications for urban governance and spatial planning. First, our analysis reveals significant spatial heterogeneity in the coupling coordination degree between day and night safety perception and crime rate, with the daytime discoordination states in Changning and Putuo Districts closely related to the high intensity commuter flows they accommodate and maintenance disparities in aging neighborhoods. This coordination imbalance significantly affects residents' daily spatial experiences, indicating an urgent need to incorporate differentiated safety perception enhancement strategies into urban renewal initiatives.

Second, although CPTED theory emphasizes crime prevention through spatial environmental design, our results reveal the potential risks of elements such as spatial

enclosure and boundary control in the absence of effective guardianship, as these design features may inadvertently create visual blind spots and escape routes (Cozens et al., 2005). Our analysis demonstrates that complex interactive effects exist between physical spatial control and social guardianship capacity, and relying solely on spatial morphology transformation cannot effectively reduce crime risk. These findings help us understand the dialectical relationship between environmental design strategies and safety governance practices in high density cities.

Based on the above findings, urban safety interventions should be tailored to the distinct risk and perception profiles of different areas in central Shanghai. First, priority should be given to improving the nighttime environment in Huangpu District. In areas with intensive commercial and tourism activities, such as the Bund and its surrounding streets, interventions should focus on streetscape maintenance, spatial order management, and sufficient and uniform lighting, particularly by reducing dark zones, uneven illumination, and visually obscured spaces. Second, crime hotspots in central and northeastern areas, as well as locations characterized by intensive leisure, nightlife, and pedestrian activity, should receive more regular nighttime patrols, visible security presence, and rapid-response deployment during peak periods to compensate for the weaker deterrent effect of static police facilities at night.

Finally, interventions should also address local mismatches between crime risk and safety perception. In areas such as Jingan and Xuhui, where safety perception is relatively high, efforts may focus on maintaining existing environmental quality while implementing targeted prevention in localized crime hotspots. In lower-crime districts such as Putuo, Changning, and Yangpu, interventions should instead focus on specific locations with low safety perception or mismatches between perceived and objective risk, rather than broadly intensifying security measures. Overall, such place- and time-specific interventions can provide a more refined and differentiated basis for urban safety governance.

4.3 Research limitations and future prospects

This study has several limitations. First, the crime data were derived from adjudicated and publicly disclosed judicial records, which may omit unreported or unprocessed incidents and introduce selection bias across offense types. Second, although the D2N model expanded nighttime streetscape samples, the use of synthetic nighttime SVI remains an important measurement limitation. Generated scenes may differ from actual nighttime streetscapes in lighting distribution, illumination conditions, pedestrian and activity patterns, color representation, and other visual features. Because the nighttime safety-perception analysis relies substantially on these generated images, such discrepancies may affect respondent's evaluations and introduce uncertainty into estimated day-night differences in safety perception.

Third, the perceived safety data were derived from a relatively limited sample, making it difficult to fully capture perceptual differences across social groups, such as those defined by age, gender, occupation, or residential experience. Fourth, temporal differences in the distribution of commuters, tourists, permanent residents, and nightlife participants may result in different exposure populations between daytime and nighttime, potentially affecting comparisons of crime rates across the two temporal contexts. Finally, this study aggregated multiple offense categories to characterize overall community-level crime risk. Although this provides a more comprehensive assessment of urban crime conditions, it may mask differences in the situational triggers and environmental dependencies of specific offenses.

To better capture the spatiotemporal dynamics of perceived safety, future research should adopt multi-source data integration approaches. First, incorporating real nighttime SVI data, such as through systematic nighttime data collection or crowdsourcing platforms, could help validate the perceptual equivalence of D2N-generated images and better reflect safety evaluations under actual lighting conditions. Second, future studies should expand the sample size and demographic coverage of perception surveys and use stratified sampling to systematically examine the moderating effects of age, gender, and socioeconomic status on perceived safety.

Third, longitudinal research designs could be adopted to track changes in perceived safety and crime patterns before and after urban renewal interventions, thereby evaluating the effectiveness of policy measures. Fourth, future research could incorporate dynamic population data, such as mobile phone signaling data, to better capture temporal variations in population exposure. Finally, future research could further distinguish among specific offense categories and examine whether different crimes respond differently to environmental and perceptual factors across daytime and nighttime contexts. Such offense-specific analyses would help identify more targeted mechanisms and support more differentiated crime-prevention strategies.

5. Conclusions

Against the backdrop of continued expansion in high density cities and the rapid growth of the nighttime economy, perceived safety was no longer merely an auxiliary indicator of crime control but a key mechanism shaping residents' nighttime mobility, spatial use, and community interaction. Focusing on Shanghai's central city, this study integrated spatiotemporal crime data from 2017 to 2019, SVI and localized survey ratings. By training a D2N model using CycleGAN to simulate nighttime crime related SVI and combining resident survey data with a GCNNWR regression framework, the study quantified daytime and nighttime levels of perceived safety and their spatial relationships with crime rate, thereby establishing a crime risk analysis framework explicitly oriented toward day night transitions.

The results showed that perceived safety at night was significantly lower than during the day and exhibited stronger spatial clustering. This perceptual disparity both overlapped with and diverged from crime distributions at the local level. Activity intensity and governance facilities also showed clear temporal differences: GAD was positively associated with crime rates, whereas the negative association of police facilities with crime weakened at night. In addition, the mediation analysis identified statistically supported indirect associations for TCI and LSU under nighttime conditions. Stronger territoriality and caretaking cues and greater lighting sufficiency and uniformity were associated with higher safety perception, which was in turn associated with lower nighttime crime risk. These findings further suggest that the relationships between CPTED-related environmental characteristics and crime risk may depend on the joint roles of perceived safety, activity intensity, and effective guardianship.

Based on these findings, the study proposed three governance pathways oriented toward urban safety. First, nighttime safety experiences should be incorporated into performance evaluation systems for the nighttime economy and livelihood governance, supported by dynamic monitoring and feedback mechanisms, particularly in high activity areas such as Huangpu District. Second, nighttime policing strategies should shift from reliance on static facilities to dynamic patrols and visible deterrence, with flexible deployment guided by nighttime pedestrian flows and incident reports. Third, place based governance should be implemented according to coupling coordination types. Areas characterized by daytime mismatch should prioritize the mitigation of environmental disorder and improvements in pedestrian continuity, while highly coupled areas should focus on eliminating blind spots and enhancing visual control, in order to reduce opportunity driven risks while improving perceived safety.

More broadly, this study had important implications for urban sustainability and social equity. The complex relationship between nighttime perceived safety and crime risk suggested that high quality development of the nighttime economy could not come at the expense of residents' sense of safety. In the context of China's policy agenda that emphasized perceived safety as a key component of public well-being while actively promoting nighttime economic development (Government, 2023, 2024), the findings provided empirical evidence for balancing economic vitality with safety experience. They also contributed to the construction of an urban safety governance framework that integrated efficiency and equity, offering practical policy insights for nighttime governance, urban regeneration, and safety planning in high density cities with a social equity orientation.

Funding declaration

We received funding from the National Social Science Fund of China under Grant No. 24BGL233.

References

Abraham, J., Kang, Y., Ceccato, V., Näsman, P., Duarte, F., Gao, S., Ljungqvist, L., Zhang, F., & Ratti, C. (2025). Crime and Visually Perceived Safety of the Built Environment: A Deep Learning Approach. *Annals of the American Association of Geographers*, 1–21.

Anderson, T. (2007). Comparison of spatial methods for measuring road accident 'hotspots': a case study of London. *Journal of maps*, *3*(1), 55–63.

Block, A. A. (2024). *Space, time, and organized crime*. Taylor & Francis.

Ceccato, V., Gaudelet, N., & Graf, G. (2022). Crime and safety in transit environments: a systematic review of the English and the French literature, 1970–2020. *Public Transport*, *14*(1), 105–153.

Cohen, L. E., & Felson, M. (1979). Social change and crime rate trends: A routine activity approach. *American sociological review*, 588–608.

Cornish, D. B., & Clarke, R. V. (2008). The rational choice perspective. *Environmental criminology and crime analysis*, *21*(10.1093).

Cozens, P. M., Saville, G., & Hillier, D. (2005). Crime prevention through environmental design (CPTED): a review and modern bibliography. *Property management*, *23*(5), 328–356.

Domínguez, P., & Asahi, K. (2023). Crime-time: how ambient light affects crime. *Journal of Economic Geography*, *23*(2), 299–317.

Dou, X. (2025). Intelligent generation method of fashion design images based on CycleGAN. *Journal of Computational Methods in Sciences and Engineering*, 14727978251364425.

Ewing, R., & Handy, S. (2009). Measuring the unmeasurable: Urban design qualities related to walkability. *Journal of Urban design*, *14*(1), 65–84.

Fan, Z., & Biljecki, F. (2024). Nighttime Street View Imagery: A new perspective for sensing urban lighting landscape. *Sustainable Cities and Society*, *116*, 105862. https://doi.org/https://doi.org/10.1016/j.scs.2024.105862

Foster, S., Knuiman, M., Hooper, P., Christian, H., & Giles-Corti, B. (2014). Do changes in residents' fear of crime impact their walking? Longitudinal results from RESIDE. *Preventive medicine*, *62*, 161–166.

Government, C. (2023). Unleash greater vitality in the nighttime economy.

Government, C. (2024). *Ensure that people enjoy a greater sense of fulfillment, happiness, and security*. Retrieved from https://www.moj.gov.cn/pub/sfbgw/zwgkztzl/2024nzt202400102/2024qglh20240219/lhjj20240219/202403/t20240307_495759.html

Government, S. (2025). *City tops China's night economy index*. english.shanghai.gov.cn. Retrieved 18.11.2025 from https://english.shanghai.gov.cn/en-PlanANightOut/20250613/63a5b5204a234f8e978771ca0b4417dc.html

Gu, H., Sui, J., Chen, P., Shan, M., & Hou, X. (2026). Safe or Unsafe? A Street-Level Analysis of the (Mis)Match Between Perceived and Objective Safety in Chaoyang District, Beijing. *ISPRS International Journal of Geo-Information*,

15(1), 13.
Haleem, M. S., Do Lee, W., Ellison, M., & Bannister, J. (2021). The 'exposed'population, violent crime in public space and the night-time economy in Manchester, UK. *European Journal on Criminal Policy and Research*, *27*(3), 335–352.
Hamim, O. F., & Ukkusuri, S. V. (2024). Towards safer streets: A framework for unveiling pedestrians' perceived road safety using street view imagery. *Accident Analysis & Prevention*, *195*, 107400.
He, Z., Gu, Y., Gong, Y., Wu, L., & Zhou, M. (2025). Analyzing the Joint Influence of Urban Facilities and Street Perception Characteristics on Street Robbery. *Journal of Geovisualization and Spatial Analysis*, *9*(1), 22. https://doi.org/10.1007/s41651-025-00222-7
Hollis-Peel, M. E., Reynald, D. M., Van Bavel, M., Elffers, H., & Welsh, B. C. (2011). Guardianship for crime prevention: A critical review of the literature. *Crime, law and social change*, *56*(1), 53–70.
Jackson, J., & Gray, E. (2010). Functional fear and public insecurities about crime. *The British Journal of Criminology*, *50*(1), 1–22.
Jeffery, C. R. (1971). Crime prevention through environmental design. *American Behavioral Scientist*, *14*(4), 598–598.
Jiang, X., Mao, Z., Zheng, Z., Lin, Z., Wang, Y., & Sheng, S. (2024). Spatio-temporal characteristics of sexual crime and influencing factors of commercial service facilities: A case study of Haining City, China. *International journal of law, crime and justice*, *76*, 100647.
Kounadi, O., Vallejo-Velázquez, M., Huang, Q., & Pődör, A. (2025). Are Places Where People Feel Safe or Unsafe Similar to Spatial Crime Patterns? Extracting the Collective Truth of the Spatial Crime Perception Gap Using Digital Sketch Maps. *Urban Science*, *9*(10), 397.
Li, X., Zhang, C., & Li, W. (2015). Does the visibility of greenery increase perceived safety in urban areas? Evidence from the place pulse 1.0 dataset. *ISPRS International Journal of Geo-Information*, *4*(3), 1166–1183.
Li, Y., Li, Y., Zhou, Y., Shi, Y., & Zhu, X. (2012). Investigation of a coupling model of coordination between urbanization and the environment. *Journal of environmental management*, *98*, 127–133.
Liska, A. E., Sanchirico, A., & Reed, M. D. (1987). Fear of crime and constrained behavior specifying and estimating a reciprocal effects model. *Soc. F.*, *66*, 827.
Liu, B., Li, F., Hou, Y., Antonio Biancardo, S., & Ma, X. (2024). Unveiling built environment impacts on traffic CO2 emissions using Geo-CNN weighted regression. *Transportation Research Part D: Transport and Environment*, *132*, 104266. https://doi.org/https://doi.org/10.1016/j.trd.2024.104266
Liu, Y., Chen, M., Wang, M., Huang, J., Thomas, F., Rahimi, K., & Mamouei, M. (2023). An interpretable machine learning framework for measuring urban perceptions from panoramic street view images. *Iscience*, *26*(3).
Liu, Z., Li, T., Ren, T., Chen, D., Li, W., & Qiu, W. (2024). Day-to-Night Street View

Image Generation for 24-Hour Urban Scene Auditing Using Generative AI. *Journal of Imaging*, *10*(5), 112.

Lorenc, T., Clayton, S., Neary, D., Whitehead, M., Petticrew, M., Thomson, H., Cummins, S., Sowden, A., & Renton, A. (2012). Crime, fear of crime, environment, and mental health and wellbeing: mapping review of theories and causal pathways. *Health & place*, *18*(4), 757–765.

Lou, S., Stancato, G., Boffi, M., Rainisio, N., Ceravolo, P., & Piga, B. E. (2024). Evaluating urban perception: Comparing Place Pulse 2.0 dataset results with images of varied field of view. In *Misura/Dismisura| Measure/Out of Measure* (pp. 471–482). Franco Angeli.

Maia, R. L., Azevedo, V., Oliveira, G. M., Guerreiro, M. S., Paulo, D., Magalhães, M., Nunes, L. M., & Sani, A. I. (2025). Urban crime and environmental triggers: A five-year analysis of reported offences in Porto's historic centre. *Cities*, *166*, 106259. https://doi.org/https://doi.org/10.1016/j.cities.2025.106259

Mandalapu, V., Elluri, L., Vyas, P., & Roy, N. (2023). Crime prediction using machine learning and deep learning: A systematic review and future directions. *Ieee Access*, *11*, 60153–60170.

Mao, Y., Yin, L., Zeng, M., Ding, J., & Song, Y. (2021). Review of empirical studies on relationship between street environment and crime. *Journal of Planning Literature*, *36*(2), 187–202.

McClanahan, W. P., Sergiou, C. S., Siezenga, A. M., Gerstner, D., Elffers, H., van der Schalk, J., & van Gelder, J.-L. (2024). Neighborhood crime reduction interventions and perceived livability: A virtual reality study on fear of crime. *Cities*, *147*, 104823.

Nasar, J. L., & Fisher, B. (1993). 'Hot spots' of fear and crime: A multi-method investigation. *Journal of environmental psychology*, *13*(3), 187–206.

Nations, U. (2025). *The Sustainable Development Goals Report*. https://unstats.un.org/sdgs/report/2025/The-Sustainable-Development-Goals-Report-2025.pdf

Navarrete-Hernandez, P., Luneke, A., Truffello, R., & Fuentes, L. (2023). Planning for fear of crime reduction: Assessing the impact of public space regeneration on safety perceptions in deprived neighborhoods. *Landscape and urban planning*, *237*, 104809.

Pain, R. (2000). Place, social relations and the fear of crime: a review. *Progress in human geography*, *24*(3), 365–387.

Pantazis, C., & Gordon, D. (2018). Poverty and crime. In *Breadline Britain in the 1990s* (pp. 115–133). Routledge.

Pradana, M. R., Dimyati, M., & Gamal, A. (2025). Harmonizing street-view semantics and spatial predictors for dominant urban visual composition modelling. *Computational Urban Science*, *5*(1), 50.

Preacher, K. J., & Hayes, A. F. (2008). Asymptotic and resampling strategies for assessing and comparing indirect effects in multiple mediator models. *Behavior research methods*, *40*(3), 879–891.

Qiu, W., Li, W., Liu, X., Zhang, Z., Li, X., & Huang, X. (2023). Subjective and

objective measures of streetscape perceptions: Relationships with property value in Shanghai. *Cities*, *132*, 104037. https://doi.org/https://doi.org/10.1016/j.cities.2022.104037

Rader, N. E., May, D. C., & Goodrum, S. (2007). An empirical assessment of the "threat of victimization:" Considering fear of crime, perceived risk, avoidance, and defensive behaviors. *Sociological Spectrum*, *27*(5), 475–505.

Roy, S., & Chowdhury, I. R. (2025). Brighter Nights, safer cities? Exploring spatial link between VIIRS nightlight and urban crime risk. *Remote Sensing Applications: Society and Environment*, *37*, 101489. https://doi.org/https://doi.org/10.1016/j.rsase.2025.101489

Sarif, N., & Roy, A. K. (2024). Measuring urban shrinkage in India using night-light data from DMSP-OLS and VIIRS-NPP satellite sensors. *Cities*, *152*, 105176. https://doi.org/https://doi.org/10.1016/j.cities.2024.105176

Shaw, C. R., & Moore, M. E. (1931). A delinquency area.

Sherman, L. W., & Weisburd, D. (1995). General deterrent effects of police patrol in crime "hot spots": A randomized, controlled trial. *Justice quarterly*, *12*(4), 625–648.

Shin, H.-S., & Woo, A. (2024). Analyzing the effects of walkable environments on nearby commercial property values based on deep learning approaches. *Cities*, *144*, 104628.

Snowden, A. J., Seligman, A. I., & Skogan, W. G. (2025). Block clubs and crime in Chicago: The transplant hypothesis. *Cities*, *158*, 105699. https://doi.org/https://doi.org/10.1016/j.cities.2024.105699

Son, D., Hyeon, T., Park, Y., & Kim, S.-N. (2023). Analysis of the relationship between nighttime illuminance and fear of crime using a quasi-controlled experiment with recorded virtual reality. *Cities*, *134*, 104184.

Stabile, C. A. (2023). *White victims, black villains: Gender, race, and crime news in US culture*. Routledge.

Suzuki, M., Mori, J., Maeda, T. N., & Ikeda, J. (2023). The economic value of urban landscapes in a suburban city of Tokyo, Japan: A semantic segmentation approach using Google Street View images. *Journal of Asian Architecture and Building Engineering*, *22*(3), 1110–1125.

Wang, R., & Rasouli, S. (2022). Contribution of streetscape features to the hedonic pricing model using Geographically Weighted Regression: Evidence from Amsterdam. *Tourism Management*, *91*, 104523.

Wang, S., Wen, H., Hui, E. C.-M., Xiao, Y., & Zhang, J. (2026). Visible environment and invisible label: Does stigmatization exist in old communities in Hangzhou, China? *Cities*, *168*, 106417. https://doi.org/https://doi.org/10.1016/j.cities.2025.106417

Wang, Y., Xiang, Y., Ma, H., Lu, Y., Chen, Z., & Qiu, W. (2026). Nightlight–nightlife interplay: Threshold effects of ambient lighting on perceived safety and physical activity at night. *International Journal of Applied Earth Observation and Geoinformation*, *147*, 105146. https://doi.org/https://doi.org/10.1016/j.jag.2026.105146

Welsh, B. C., & Farrington, D. P. (2008). Effects of improved street lighting on crime. *Campbell systematic reviews*, *4*(1), 1–51.

Woo, A., Han, J., Shin, H., & Lee, S. (2024). Economic benefits of urban streetscapes: Analyzing the interrelationships between visual street environments and single-family property values in Seoul, Korea. *Applied geography*, *163*, 103182.

Xu, L., Tao, Y., Yu, H., Du, W., Chen, Z., & Chen, N. (2025). Geographically weighted regression with convolutional neural networks to integrate attribute similarity and spatial proximity. *International Journal of Geographical Information Science*, 1–26.

Ye, X., Wang, Y., Dai, J., & Qiu, W. (2025). Generated nighttime street view image to inform perceived safety divergence between day and night in high density cities: A case study in Hong Kong. *Journal of Urban Management*, *14*(2), 379–401. https://doi.org/https://doi.org/10.1016/j.jum.2024.11.006

You, Y., Lai, W., & Huang, L. (2026). Measuring Street Spatial Form Using Street View Imagery and Computer Vision: A Case Study of the Greater Bay Area, China. *Journal of Geovisualization and Spatial Analysis*, *10*(1), 20. https://doi.org/10.1007/s41651-026-00262-7

Yu, P., Yang, X., Guo, Q., Guan, J., & Chen, G. (2025). Spatial distribution characteristics and influencing factors of China martial arts schools based on Baidu map API. *PLoS One*, *20*(3), e0314588.

Zhang, F., Fan, Z., Kang, Y., Hu, Y., & Ratti, C. (2021). “Perception bias”: Deciphering a mismatch between urban crime and perception of safety. *Landscape and urban planning*, *207*, 104003.

Zhang, Y., Kwan, M.-P., & Fang, L. (2025). An LLM driven dataset on the spatiotemporal distributions of street and neighborhood crime in China. *Scientific Data*, *12*(1), 467. https://doi.org/10.1038/s41597-025-04757-8

Zhou, H., Liu, L., Wang, J., Wilson, K., Lan, M., & Gu, X. (2024). A multiscale assessment of the impact of perceived safety from street view imagery on street crime. *Annals of the American Association of Geographers*, *114*(1), 69–90.